Published in final edited form as:
Glia. 2006 April 1; 53(5): 529–537. doi:10.1002/glia.20297.

Upregulation of the Stress-Associated Gene p8 in Mouse Models of Demyelination and in Multiple Sclerosis Tissues

Sheila R. Plant[1,2], **Ying Wang**[1,3], **Sophie Vasseur**[4], **J. Cameron Thrash**[5], **Eileen J. Mcmahon**[6], **Daniel T. Bergstralh**[1], **Heather A. Arnett**[7], **Stephen D. Miller**[6], **Monica J. Carson**[5], **Juan L. Iovanna**[4], and **Jenny P-Y. Ting**[1,2,3,*]

1*Lineberger Comprehensive Cancer Center, University of North Carolina, Chapel Hill, North Carolina*

2*Neuroscience Center, University of North Carolina, Chapel Hill, North Carolina*

3*Department of Microbiology-Immunology, University of North Carolina, Chapel Hill, North Carolina*

4*Department of Stress Cellulaire, Centre de Recherche INSERM, EMI 0116, Marseilles, France*

5*Division of Biomedical Sciences, University of California, Riverside, California*

6*Department of Microbiology-Immunology and the Interdepartmental Immunobiology Center, Northwestern University Medical School, Chicago, Illinois*

7*Department of Inflammation, Amgen Corporation, Seattle, Washington*

Abstract

Cuprizone-induced demyelination is a mouse model of multiple sclerosis (MS) as cuprizone-fed mice exhibit neuroin-flammation and demyelination in the brain. Upon removal of cuprizone from the diet, inflammation is resolved and reparative remyelination occurs. In an Affymetrix Gene-Chip analysis, the stress-associated gene p8 was strongly upregulated (>10×) during cuprizone-induced demyelination but not remyelination. We verified this upregulation (>15×) of p8 in the CNS during demyelination by real-time polymerase chain reaction (PCR). This upregulation is brain-specific, as p8 is not elevated in the liver, lung, kidney, spleen, and heart of cuprizone-treated mice. We also localized the cellular source of p8 during cuprizone treatment, and further found elevated expression during embryogenesis but not in normal adult brain. Compared with wild-type controls, the death of oligodendrocytes in $p8^{-/-}$ mice is delayed, as is microglial recruitment to areas of demyelination. The corpus callosum of $p8^{-/-}$ mice demyelinates at a slower rate than wild-type mice, suggesting that p8 exacerbates CNS inflammation and demyelination. Enhanced expression of p8 is also observed in the spinal cords of mice with acute experimental autoimmune encephalomyelitis (EAE) induced by $PLP_{139–151}$ peptide (10×). Increased expression is detected during disease onset and expression wanes during the remission phase. Finally, p8 is found upregulated (8×) in post-mortem tissue from MS patients and is higher in the plaque tissue compared with adjacent normal-appearing white and gray matter. Thus, p8 is an excellent candidate as a novel biomarker of demyelination.

Keywords

glia; multiple sclerosis; cuprizone; biomarker; EAE

*Correspondence to: Jenny P-Y. Ting, Lineberger Comprehensive Cancer Center, CB# 7295, University of North Carolina, Chapel Hill, NC 27599. E-mail: panyun@med.unc.edu.

INTRODUCTION

p8 is a small ubiquitous protein of 80 amino acids identified upon its strong but transient upregulation in pancreatic acinar cells during experimental acute pancreatitis, development and regeneration (Mallo et al., 1997). Expression of p8 is upregulated by a wide range of cellular stressors, including pro-apoptotic agents, lipopolysaccharide, and simply changing culture media (Jiang et al., 1999; Garcia-Montero et al., 2001). The same molecule was independently discovered and named candidate of metastasis 1 (com1) in a screen of breast cancer cells and is highly upregulated and even required for tumor development and progression (Ree et al., 1999, 2000; Vasseur et al., 2002a,b; Su et al., 2001b). In pancreatic cancer, p8 overexpression inversely correlated with apoptosis (Su et al., 2001a), suggesting that dying cells are not expressing p8. Thus, p8 may have pro-survival properties. p8 is likely a DNA-binding protein, although its DNA-binding capacity is found to be weak, and it has structural characteristics shared with the high-mobility group (HMG) proteins, thus strongly implicating its role in transcriptional regulation (Encinar et al., 2001).

The role of p8 in the brain has not been established. p8 mRNA expression in normal rat and human brain was barely detectable (Mallo et al., 1997; Vasseur et al., 1999). Induction of p8 was not observed in the brain after systemic injection of lipopolysaccharide (LPS) (Jiang et al., 1999). Recently, the level of p8 was found to correlate with pituitary gland tumor development, implicating p8 in tumorigenesis of the pituitary gland in the brain (Mohammad et al., 2004).

During cuprizone-induced demyelination, we discovered a profound upregulation of p8 following inflammation and demyelination in the mouse brain by Affymetrix GeneChip analysis (Arnett et al., 2003). Cuprizone is a copper chelator that, when given in small doses (0.2%) in the feed of mice, acts as a neurotoxin that specifically induces the death of oligodendrocytes and causes inflammation in areas of resulting demyelination (Matsushima and Morell, 2001). The effect is reversible such that its removal from the diet permits remyelination and a reduction in inflammation. Thus, cuprizone-induced demyelination permits analysis of inflammation, demyelination, and remyelination. The lesions that occur in the brains of cuprizone-treated mice are similar to type III and type IV MS lesions (Lucchinetti et al., 2000). An advantage of the cuprizone model is the predictability of lesion location. Large tracts of myelinated fibers, specifically the corpus callosum and the cerebral peduncles, are the normal target of cuprizone-induced demyelination (Matsushima and Morell, 2001). In this model, focal inflammation and demyelination occurs in the brain however T lymphocytes do not play a role (Hiremath et al., 1998; Matsushima and Morell, 2001). RAG-$1^{-/-}$ mice, which lack T and B cells, respond similarly to wild-type controls upon cuprizone treatment (Arnett et al., 2001).

We show that the upregulation of p8 is restricted to the brain during cuprizone-induced demyelination and is not a general response found in other tissues. p8 is primarily upregulated in microglia, although during the peak of inflammation, it can be found elevated in other cells as well. CNS-derived p8 upregulation is not limited to the cuprizone model and occurs during the height of experimental autoimmune encephalomyelitis. Most significantly, p8 is greatly elevated in multiple sclerosis plaques. Together with a functional analysis of p8 during inflammatory demyelinating disease using mice lacking the gene, these results suggest that p8 is a strong biomarker candidate for demyelination.

MATERIALS AND METHODS

Animals and Treatment

Mice lacking $p8^{-/-}$ and wild-type control mice ($p8^{+/+}$) were bred to the C57BL/6 background (8th generation). All mice were 8–10 weeks of age before the start of cuprizone treatment. Male $p8^{-/-}$ and $p8^{+/+}$ mice were fed 0.2% cuprizone [oxalic bis(cyclohexylidenehydrazide)] (Aldrich, St. Louis, MI) for 2, 3, 3.5, 4, or 5 weeks.

SJL female mice were purchased from Harlan-Sprague-Dawley (Indianapolis, IN). Induction of experimental autoimmune encephalomyelitis (EAE) was carried out according to standard protocol at 6–8 weeks of age. Mice were primed subcutaneously with an emulsion containing 100 μl of incomplete Freund's adjuvant (Difco) supplemented with 200 μg *Mycobacterium* tuberculosis H37Ra (Difco, Kansas City, MO) and 100 lg of either $PLP_{139–151}$ (HSLGKWLGHPDKF) or $OVA_{323–339}$ (ISQAVHAAHAEI-NEAGR) distributed over three spots on the flank. Clinical disease was monitored as previously described (McRae et al., 1995). Three mice were sacrificed at each clinical time point; preclinical (right before onset of clinical symptoms), peak of acute disease, and remission.

Tissue Preparation and Histopathological Analysis

Brains from cuprizone-treated mice were paraffin embedded, and coronal sections were cut at the fornix region of the corpus callosum as detailed (Arnett et al., 2001). To examine myelination, sections were stained by Luxol fast blue-periodic acid Schiff (LFB-PAS; Sigma, St. Louis, MO). Sections were read by three double-blinded readers and graded on a scale from 0 (complete myelination) to 3 (complete demyelination).

In Situ Hybridization

C57BL/6 mice were perfused with RNase-free phosphate-buffered saline (PBS) and then 4% PFA. Brains were incubated in fixative until mounted for cryosectioning. Detection of mRNA for p8 was performed by in situ hybridization as described previously (Schmid et al., 2002). Expression of p8 and beta-actin were quantitated using NIH Image 1.62 software, and relative abundance of p8 was determined. For double-labeling experiments, immunohistochemistry with either GFAP, NeuN, or CNPase antibodies or tomato lectin was performed to identify astrocytes, neurons, oligodendrocytes or microglia/macrophages respectively.

Immunohistochemistry

Mature oligodendrocytes were detected by the GSTπ primary antibody as described (Plant et al., 2005). Microglia/macrophages were detected with RCA-1 (Vector) as described.

Tissue and RNA Processing

SJL mice were anesthetized and perfused with PBS. The brains and spinal cords were harvested and snap frozen on dry ice. They were then stored at −80° C until further processing. Tissue was homogenized by forcing through a metal screen. Total RNA was isolated using Trizol according to the manufacturer's instructions (Invitrogen). RNA was then treated with DNase I (Invitrogen) to eliminate any DNA contamination.

C57BL/6 mice were lethally anesthetized, and organs (brain, liver, kidney, heart, spleen, lung) were immediately removed and stored in RNALater until further processing (Qiagen, Valencia, CA). Total RNA was isolated from a dissected region of C57BL/6 wild-type mouse brains containing the corpus callosum. RNA isolations were performed using the Qiagen RNeasy kit.

Multiple Sclerosis Tissues

Frozen postmortem tissue samples were obtained from the Human Brain and Spinal Fluid Resource Center (Los Angeles, CA). Tissue samples were from the frontal, parietal and occipital brain regions of three patients previously diagnosed with multiple sclerosis. Normal-appearing white matter (NAWM), normal-appearing gray matter (NAGM) and an adjacent plaque were dissected from each region. RNA was isolated using the Qiagen RNeasy kit.

Real-Time Quantitative RT-PCR

TaqMan 5′ nuclease real-time PCR assays were performed using an ABI Prism 7900 sequence-detection system (PE Applied Biosystems, Foster City, CA) using primers for p8 designed to span intron–exon junctions to differentiate between cDNA and genomic DNA. Primers and probe used to detect mouse p8 were as follows: 5′ primer, TTCCCCCACAGTTCTTTTGG; 3′ primer, GGCAAGATGGGAGCAAGAAG; probe, Fam-CTGTCTTCCTAGCTCTG-CCCGTCTACCC-Tamra. Primers and probe used to detect human p8 were as follows: 5′ primer, CGCTGAGAC-AGAGCTGGAGAT; 3′ primer, GCAAGCCGGCCTGGAT; probe, Fam-AGGCCAGACCATGGACACTACACCCA-Tamra. Primers and probe for 18S ribosomal RNA were 5′ primer, GCTGCTGGCACCAGACTT; 3′ primer, CGGCTACCACATCCAAGG; probe, Fam-CAAATTACCCACTCCCGACCCG-Tamra. Thermal cycle parameters were optimized to 2 min at 50°C, 2 min at 95°C, and 40 cycles comprising denaturation at 95°C for 15 s and annealing–extension at 56°C for 1.5 min. Reactions for 18S were performed alongside p8 during each experiment and used to normalize for amounts of cDNA.

Isolation of Peritoneal Macrophages and Cell Death Assay

Following CO_2 asphyxiation, the peritoneal cavity was flushed with PBS using a 27-gauge needle. Approximately 7 ml of peritoneal fluid was recovered from each mouse. Peritoneal lavage fluid from 4 $p8^{-/-}$ and 4 $p8^{+/+}$ mice were pooled and 75,000 cells/well were plated in 96-well microtiter plates and allowed to adhere overnight. Cells were washed and treated as indicated in 200 µl of new media. Each treatment was performed in triplicate. After 72 h, 50 µl of serum-free media containing 1 µg/ml XTT and 25 mM phenazine methosulfate was added to each well. Plates were read at 450 nm after 4 h of incubation. Viability was calculated as the percentage of color change relative to untreated control. Error bars represent the standard deviation for each triplicate set.

Statistical Analysis

Unpaired Student's *t*-tests were used to statistically evaluate significant differences. Data are expressed as mean ± SEM.

RESULTS

Upregulation of p8 During Cuprizone-Induced Inflammation and Demyelination

The treatment of C57BL/6 mice with 0.2% cuprizone in the diet induces neuro-inflammation and demyelination in a predictable time course. Gross demyelination, loss of mature oligodendrocytes, microglial/macrophage and astrocyte activation and recruitment to areas of demyelination are observed consistently in the large myelinated fiber tracts, including the corpus callosum. While these processes begin within 1 week of treatment (Matsushima and Morell, 2001), significant changes in cell numbers at the corpus callosum are typically not observed until about 3 weeks (Fig. 1). Microglia and astrocyte recruitment to areas of demyelination is greatest around weeks 4–5 in wild-type mice. Demyelination is complete and no mature oligodendrocytes are detected in the corpus callosum after 5 weeks (Fig. 1).

Using an Affymetrix GeneChip analysis of cuprizonetreated mouse brain tissue (Arnett et al., 2003), we found p8 upregulated 11-fold over p8 levels in untreated brain (Fig. 2). Real-time quantitative PCR analysis was performed on cDNA from mouse brain tissue before and after cuprizone treatment to verify this finding. Compared with untreated brain, p8 was upregulated about 10× within 1 week of cuprizone treatment and peaked at 3 weeks of treatment (15×) (Fig. 3A). p8 remained elevated at 5 weeks of treatment, and then declined during the remyelination phase at weeks 6 and 7. As reported, p8 was downregulated on the GeneChip after mice were returned to a normal diet which allows for remyelination to proceed (Fig. 2), and the real-time PCR analysis verified these data (Fig. 3). Thus, upregulation of p8 is coincident with the active inflammatory demyelinating phase and not with remyelination.

To determine whether p8 was upregulated in other body organs during cuprizone treatment, real-time PCR analysis of p8 in liver, kidney, heart, spleen, and lung tissues was performed. p8 levels vary widely from organ to organ; however, they remained steady in these tissues during or after cuprizone treatment (Fig. 3B–F). Thus, p8 upregulation upon cuprizone treatment is specific to the brain.

Early Developmental p8 Expression

As reports of p8 expression in the brain are minimal, we investigated the presence of p8 in the brain during development and under normal conditions. Northern blot analysis for p8, and β-actin as a control, was performed on mRNA from brain and liver tissues from mice at various ages. In the brain, p8 mRNA levels are high at embryonic day 14 (E14) and highest at E16 and E18 (Fig. 4A, and quantitation in Fig. 4B). Strikingly, this is the period of greatest programmed cell death in the embryonic mouse brain where an estimated 50–70% of cortical cells are dying (Blaschke et al., 1996). In addition, extensive microglial activation occurs during this phase in the cerebral cortex (Upender and Naegele, 1999). Considering that p8 is often upregulated in cells undergoing stress, it is possible the cells undergoing programmed cell death and/or the activated microglia are producing high levels of p8. Following birth, p8 mRNA levels are barely detectable and stabilize at low levels starting at postnatal day 20 through adulthood. Interestingly, the level of p8 expression in the CNS is lower than that seen in the adult liver. In contrast, p8 in the embryonic liver is much lower than p8 levels in the adult liver (Fig. 4). These data coincide with other reports that p8 levels are very low to undetectable in the rat and human adult brain but show that brain p8 expression is high during embryogenesis (Mallo et al., 1997;Vasseur et al., 1999).

Localization of p8 During Inflammation

To localize p8 mRNA expression in the brain, in situ hybridization was performed with an antisense riboprobe specific for p8 mRNA. The sense p8 probe showed no staining (Fig. 5A, sense). In the untreated state, it was very difficult to determine the location of p8 expression as levels were very low (Fig. 5A). A dramatic induction of p8 mRNA is detected by 2 weeks of cuprizone treatment and the expression seems to be restricted to the hippocampus and corpus callosum (arrow). By 4 weeks of treatment, very high levels of p8 were expressed throughout the entire brain demonstrating a dramatic global upregulation of p8 throughout the entire mouse brain. Interestingly, even though the mice remain on cuprizone for a full 6 weeks, p8 overexpression subsided by 5 weeks and localized more specifically to the corpus callosum region where most pathology actually occurs (Fig. 5A, arrow). Cuprizone specifically targets oligodendrocytes in the brain causing massive demyelination in the corpus callosum and other large myelinated fiber tracts. In addition, a predictable inflammatory response occurs in which large numbers of microglia, macrophages, and astrocytes enter the corpus callosum (Matsushima and Morell, 2001;Plant et al., 2005). Considering the extensive trauma that occurs at the corpus callosum, it is not surprising to find many cells in the corpus callosum expressing p8. However, the reason that p8 upregulation initiates in the hippocampus is unknown.

To determine the $p8^{+}$ cell type in the brain, in situ hybridization was coupled with immunohistochemistry. Tomato lectin was used to label microglia and macrophages while antibodies specific for CNPase-labeled oligodendrocytes, GFAP-labeled astrocytes, and NeuN-labeled neurons. After 2 weeks of cuprizone treatment, lectin-positive microglia/ macrophages were highly positive for p8, while the level of p8 in oligodendrocyte, neurons and astrocytes was very low (data not shown). At 4 weeks, p8 mRNA was expressed by all cell types in the brain, but the level of p8 in microglia (Fig. 5B,a,b) was significantly greater than that in oligodendrocytes (Fig. 5B,c,d) or other cell types (data not shown). We conclude that p8 is most prominently, but not exclusively, expressed by microglia and macrophages during cuprizone-induced inflammation and demyelination.

Delay in Demyelination Without p8

To investigate the functional effect of p8 during cuprizone-induced inflammation and demyelination, we induced demyelination in mice lacking p8. Both $p8^{+/+}$ and $p8^{-/-}$ mice were fed 0.2% cuprizone in their diet for 0, 2, 3, 3.5, 4, or 5 weeks before sacrifice. Paraffin brain sections were stained with LFB-PAS. The extent of demyelination was assessed at midline corpus callosum at the level of the fornix on a scale from 0 (complete normal myelin) to 3 (complete demyelination). Scores from each individual mouse were plotted (Fig. 6). Although $p8^{-/-}$ mice showed less overall demyelination compared with wild-type mice at the 2- and 3-week time points, the differences are not statistically significant. However, after 3.5 weeks of treatment, wild-type mice displayed significantly more demyelination than did $p8^{-/-}$ mice ($P < 0.0001$). By 4 and 5 weeks of cuprizone treatment, almost all mice were fully demyelinated such that no differences were seen between wild-type and $p8^{-/-}$ mice. Thus, p8 has a significant but transient role in exacerbating the inflammatory demyelinating process in the brain.

Moderate Delay in Oligodendrocyte Death in $p8^{-/-}$ Mice

To verify the LFB data, immunohistochemistry to detect mature oligodendrocytes was performed on adjacent paraffin sections using the GSTπ primary antibody. Similar to the LFB data, 0, 2, or 3-week-treated brains from wild-type and $p8^{-/-}$ mice have similar numbers of mature oligodendrocytes. After 3.5 weeks of treatment, more GSTπ-positive oligodendrocytes were present in the corpus callosum of $p8^{-/-}$ mice compared with wild-type mice ($P = 0.14$) (Fig. 7A). Mature oligodendrocytes in both strains of mice were almost depleted by 4 weeks of cuprizone treatment.

Delayed Microglia/Macrophage Recruitment to Corpus Callosum in $p8^{-/-}$ Mice

To explore the possible mechanism accounting for the delay in oligodendrocyte death and demyelination in the corpus callosum of $p8^{-/-}$ mice, we investigated the effects of p8 on microglial and macrophage recruitment to the demyelinating region. RCA-1 lectin was used to mark microglia and peripheral macrophages. Lectin-positive cells at midline corpus callosum were quantitated in double-blind fashion. Significantly more microglia/macrophages were found in wild-type mice compared with $p8^{-/-}$ mice ($P < 0.04$) (Fig. 7B). It is possible that $p8^{-/-}$ microglia/ macrophages are less responsive to activation and recruitment signals to areas of demyelination. They may also undergo apoptosis more readily. Alternatively, the reduced oligodendrocyte cells in $p8^{-/-}$ mice may in turn lessen inflammation and reduce microglial recruitment.

Apoptosis of Macrophages is Unchanged in $p8^{-/-}$ Mice

To assess whether p8 has any role in apoptosis or cell death, $p8^{-/-}$ and $p8^{+/+}$ macrophages were examined for susceptibility to cell death. Peritoneal macrophages were isolated instead of microglia because the latter are very difficult to isolate from mice. Cells were exposed to a number of pro-apoptotic stimuli: staurosporine, Taxol, and ultraviolet (UV) irradiation. Cell

viability was measured 72 h later using the XTT assay. No difference in susceptibility to these agents was determined, suggesting that p8 is not involved in defense against apoptosis of macrophages (Fig. 7C). Thus the reduced numbers of $p8^{-/-}$ macrophages at the site of inflammation and demyelination (Fig. 7B) is not due to enhanced macrophage cell death. Thus, while we cannot say for certain why $p8^{-/-}$ microglia/macrophages are slower to accumulate at the corpus callosum, $p8^{-/-}$ microglia and macrophages probably do not have a greater susceptibility to apoptose during cuprizone-induced demyelination.

Upregulation of p8 in Experimental Autoimmune Encephalomyelitis

To assess whether the dramatic upregulation of microglial p8 seen during cuprizone-induced demyelination occurs in another model of demyelination, we used the EAE model. This model is well studied and is a prototype of T-cell-mediated demyelination. SJL mice were treated with $PLP_{139–151}$ and adjuvant to induce EAE, then sacrificed at a preclinical time point, at the peak of disease, or during remission. Real-time PCR analysis was performed using cDNA generated from these samples. No difference in p8 mRNA levels between control OVA-treated and $PLP_{139–151}$-treated mice was found, and no change in p8 levels was found during the clinical time course of $PLP_{139–151}$-treated mice (Fig. 8A). In the spinal cord, preclinical samples also expressed the same amount of p8 as OVA-treated samples. However, a significant upregulation of p8 (10-fold) was detected at the peak of disease in PLP-treated mice (Fig. 8B). Levels of p8 mRNA decreased during the remission stage. We believe that the differences in p8 expression in brain and spinal cord are due to the fact that in EAE, pathology begins in the caudal spinal cord and gradually moves in the rostral direction with minimal pathology in the brain (Oldendorf and Towner, 1974;Cross et al., 1993). In addition, the severity of EAE is typically much greater in the spinal cord than the brain, which could account for the differential expression of p8 in the spinal cord and brain (Leibowitz and Kennedy, 1972;Simmons et al., 1982).

Upregulation of p8 in Multiple Sclerosis

To assess the translational relevance of the above findings, we investigated the involvement of human p8 in MS. Plaque samples from the frontal, parietal, and occipital lobes of each of three MS patients were used to generate cDNA. Adjacent normal-appearing white matter (NAWM) and adjacent normal-appearing gray matter (NAGM) were studied. Real-time PCR analysis revealed a dramatic upregulation of p8 in all plaque tissues tested compared with NAWM and NAGM (Fig. 9). Although there was significant degree of sample-to-sample variability, p8 levels were always higher in the plaque tissue than in the adjacent NAWM and NAGM.

DISCUSSION

As a means to locate novel mediators of demyelination and remyelination, we used an unbiased cDNA profiling approach to identify genes which exhibit significantly altered expression during the demyelination and remyelination phases of the cuprizone disease model (Arnett et al., 2003). Affymetrix array analysis identified p8 as one of the most profoundly affected genes during the demyelination phase, and this was verified in several ways. First, it is selectively and profoundly enhanced during demyelination but not during remyelination. Second, during cuprizone treatment, p8 is selectively enhanced in the brain but not in other tissues. Third, p8 is elevated in brains from cuprizone-treated mice, in the afflicted spinal cords of mice with EAE and in postmortem human MS plaques. Functional analysis of p8-deficient mice further confirmed a significant, albeit transitory, role of p8 in enhancing the extent of demyelination. Thus, this represents the first report linking p8 to the demyelination phase of neurodegenerative disorders.

An initial concern is whether p8 upregulation in the brain is simply a nonspecific response to cuprizone. This is clearly not the case, as other tissues surveyed from cuprizone-treated mice do not exhibit enhanced p8 expression, although their basal level of p8 expression varied widely. Furthermore, we have shown that the enhanced expression of p8 occurs in other relevant instances of demyelination. p8 is elevated 10-fold in the spinal cord of mice at the peak of symptoms in $PLP_{139–151}$-induced EAE (Fig. 8B). While this upregulation was found in the spinal cord and not the brain, this may be due to the lack of significant pathology in the brains of these mice after treatment. Even more importantly, we found p8 to be elevated in MS plaques relative to the adjacent normal-appearing white and gray matter (Fig. 9). This was observed in a variety of plaques found in all lobes of the brain and in both genders from patients at different ages. With the ability to study the role of p8 in different models of MS, cuprizone-induced demyelination and EAE, identifying a role for p8 in demyelination may be possible. As p8 appears to bind DNA and probably acts as a transcription factor, it will be important to identify the gene targets that are subjected to regulation by p8. Either p8 or its targets may unveil novel biologic and regulatory processes that may affect the outcome of demyelination.

We next investigated which cell types express p8 and how p8 upregulation may affect the course of demyelination. In situ hybridization during early treatment demonstrates a relatively restricted upregulation of p8 that could be attributed to the microglial population (week 2). However, by 4 weeks of cuprizone treatment, there is a dramatic upregulation of p8 throughout the entire brain. While microglia/macrophages clearly express p8 at a very high level at 4 weeks, it appears that p8 is widely expressed by oligodendrocytes, astrocytes and neurons as well, but at a significantly lower level. In the cuprizone model, this is the time point when many of the mature oligodendrocytes are dead or dying, yet concomitantly oligodendrocyte progenitors are increasing in number, and microglia/macrophages and astrocytes are highly activated and recruited to areas of demyelination (Matsushima and Morell, 2001) (Fig. 1). This corresponds with a previous finding that the overexpression of p8 accompanied and enhanced cellular proliferation (Vasseur et al., 1999). Indeed, the analysis of mice deficient in p8 show that microglial/macrophage accumulation at the demyelination site appears to be significantly reduced by the absence of p8 (Fig. 7B). The reduced microglial accumulation likely contributes to a decrease in the overall inflammatory environment and in the loss of oligodendrocytes.

Currently, the link, if any, between the upregulation of p8 in numerous types of human cancers and its upregulation during demyelination is unclear (Ree et al., 2000; Su et al., 2001b). It has been noted that the development of metastasis in target organs correlated with p8 expression (Ree et al., 1999). Tumor establishment through the introduction of the rasV12 mutated protein and the E1A do not occur in embryonic fibroblasts derived from mice lacking p8 (Vasseur et al., 2002a), suggesting the requirement of p8 for the development of cancer. It has been hypothesized that p8 expression in cancer is simply a response to the stressful environment engendered by metastatic cancer (Iovanna, 2002). In addition to tumor-induced stress, simply changing the culture media of cells induced upregulation of p8 as did exposure to lipopolysaccharide and pro-apoptotic agents (Jiang et al., 1999; Garcia-Montero et al., 2001). By extension to the CNS, while p8 expression is not significant in normal adult brain tissues, p8 is induced in the embryonic mouse brain during development, correlating with the period of massive programmed cell death and growth. In an inflammatory, demyelinating adult brain, cells are exposed to an unusual environment that may induce a stress response causing p8 induction.

In summary, this report is the first to show a selective enhancement of p8 in the affected brains of different demyelination models and of humans afflicted with MS. Functional analysis shows that p8 expression can exacerbate the extent of demyelination, cause an enhanced presence of microglial cells and a concomitant decrease in oligodendrocytes. The brain-specific elevation

of p8, as well as its enhancement during demyelination, suggests that p8 may serve as a marker for neuroinflammation and/or demyelination.

ACKNOWLEDGMENTS

Tissue specimens were obtained from the Human Brain and Spinal Fluid Resource Center, VAMC, Los Angeles, CA 90073, sponsored by NINDS/NIMH, National Multiple Sclerosis Society, VA Greater Los Angeles Healthcare System, 11301 Wilshire Blvd. Los Angeles, CA 90073, and Veterans Health Services and Research Administration, Department of Veterans Affairs. This work was supported by NIH grants NS34190 (to J.P.-Y.T.), NS39508 (to M.C.), NS045735 (to M.C.) and by NMSS grant RG1785 (to J.PY. T.).

Grant sponsor: National Institutes of Health; Grant number: NS34190; Grant number: NS39508; Grant number: NS045735: Grant sponsor: National Multiple Sclerosis Society; Grant number: RG1785.

REFERENCES

Arnett HA, Mason J, Marino M, Suzuki K, Matsushima GK, Ting JP. TNF alpha promotes proliferation of oligodendrocyte progenitors and remyelination. Nat Neurosci 2001;4:1116–1122. [PubMed: 11600888]

Arnett HA, Wang Y, Matsushima GK, Suzuki K, Ting JP. Functional genomic analysis of remyelination reveals importance of inflammation in oligodendrocyte regeneration. J Neurosci 2003;23:9824–9232. [PubMed: 14586011]

Blaschke AJ, Staley K, Chun J. Widespread programmed cell death in proliferative and postmitotic regions of the fetal cerebral cortex. Development 1996;122:1165–1174. [PubMed: 8620843]

Cross AH, O'Mara T, Raine CS. Chronologic localization of myelin-reactive cells in the lesions of relapsing EAE: implications for the study of multiple sclerosis. Neurology 1993;43:1028–1033. [PubMed: 7684116]

Encinar JA, Mallo GV, Mizyrycki C, Giono L, Gonzalez-Ros JM, Rico M, Canepa E, Moreno S, Neira JL, Iovanna JL. Human p8 is a HMG-I/Y-like protein with DNA binding activity enhanced by phosphorylation. J Biol Chem 2001;276:2742–2751. [PubMed: 11056169]

Garcia-Montero A, Vasseur S, Mallo GV, Soubeyran P, Dagorn JC, Iovanna JL. Expression of the stress-induced p8 mRNA is transiently activated after culture medium change. Eur J Cell Biol 2001;80:720–725. [PubMed: 11824791]

Hiremath MM, Saito Y, Knapp GW, Ting JP, Suzuki K, Matsushima GK. Microglial/macrophage accumulation during cuprizone-induced demyelination in C57BL/6 mice. J Neuroimmunol 1998;92:38–49. [PubMed: 9916878]

Iovanna JL. Expression of the stress-associated protein p8 is a requisite for tumor development. Int J Gastrointest Cancer 2002;31:89–98. [PubMed: 12622419]

Jiang YF, Vaccaro MI, Fiedler F, Calvo EL, Iovanna JL. Lipopoly-saccharides induce p8 mRNA expression in vivo and in vitro. Biochem Biophys Res Commun 1999;260:686–690. [PubMed: 10403827]

Leibowitz S, Kennedy L. Cerebral vascular permeability and cellular infiltration in experimental allergic encephalomyelitis. Immunology 1972;22:859–869. [PubMed: 5021707]

Lucchinetti C, Bruck W, Parisi J, Scheithauer B, Rodriguez M, Lassmann H. Heterogeneity of multiple sclerosis lesions: implications for the pathogenesis of demyelination. Ann Neurol 2000;47:707–717. [PubMed: 10852536]

Mallo GV, Fiedler F, Calvo EL, Ortiz EM, Vasseur S, Keim V, Morisset J, Iovanna JL. Cloning and expression of the rat p8 cDNA, a new gene activated in pancreas during the acute phase of pancreatitis, pancreatic development, and regeneration, and which promotes cellular growth. J Biol Chem 1997;272:32360–32369. [PubMed: 9405444]

Matsushima GK, Morell P. The neurotoxicant, cuprizone, as a model to study demyelination and remyelination in the central nervous system. Brain Pathol 2001;11:107–116. [PubMed: 11145196]

McRae BL, Vanderlugt CL, Dal Canto MC, Miller SD. Functional evidence for epitope spreading in the relapsing pathology of experimental autoimmune encephalomyelitis. J Exp Med 1995;182:75–85. [PubMed: 7540658]

Mohammad HP, Seachrist DD, Quirk CC, Nilson JH. Reexpression of p8 contributes to tumorigenic properties of pituitary cells and appears in a subset of prolactinomas in transgenic mice that hypersecrete luteinizing hormone. Mol Endocrinol 2004;18:2583–2593. [PubMed: 15243129]

Oldendorf WH, Towner HF. Blood-brain barrier and DNA changes during the evolution of experimental allergic encephalomyelitis. J Neuropathol Exp Neurol 1974;33:616–631. [PubMed: 4436687]

Plant S, Arnett H, Ting J. Astroglial-derived lymphotoxin-alpha exacerbates inflammation and demyelination, but not remyelination. Glia 2005;49:1–14. [PubMed: 15382206]

Ree AH, Pacheco MM, Tvermyr M, Fodstad O, Brentani MM. Expression of a novel factor, com1, in early tumor progression of breast cancer. Clin Cancer Res 2000;6:1778–1783. [PubMed: 10815897]

Ree AH, Tvermyr M, Engebraaten O, Rooman M, Rosok O, Hovig E, Meza-Zepeda LA, Bruland OS, Fodstad O. Expression of a novel factor in human breast cancer cells with metastatic potential. Cancer Res 1999;59:4675–4680. [PubMed: 10493524]

Schmid CD, Sautkulis LN, Danielson PE, Cooper J, Hasel KW, Hilbush BS, Sutcliffe JG, Carson MJ. Heterogeneous expression of the triggering receptor expressed on myeloid cells-2 on adult murine microglia. J Neurochem 2002;83:1309–1320. [PubMed: 12472885]

Simmons RD, Bernard CC, Singer G, Carnegie PR. Experimental autoimmune encephalomyelitis. An anatomically-based explanation of clinical progression in rodents. J Neuroimmunol 1982;3:307–318. [PubMed: 7174784]

Su SB, Motoo Y, Iovanna JL, Berthezene P, Xie MJ, Mouri H, Ohtsubo K, Matsubara F, Sawabu N. Overexpression of p8 is inversely correlated with apoptosis in pancreatic cancer. Clin Cancer Res 2001a;7:1320–1324. [PubMed: 11350901]

Su SB, Motoo Y, Iovanna JL, Xie MJ, Mouri H, Ohtsubo K, Yamaguchi Y, Watanabe H, Okai T, Matsubara F, et al. Expression of p8 in human pancreatic cancer. Clin Cancer Res 2001b;7:309–313. [PubMed: 11234885]

Upender MB, Naegele JR. Activation of microglia during developmentally regulated cell death in the cerebral cortex. Dev Neurosci 1999;21:491–505. [PubMed: 10640867]

Vasseur S, Hoffmeister A, Garcia S, Bagnis C, Dagorn JC, Iovanna JL. p8 is critical for tumour development induced by rasV12 mutated protein and E1A oncogene. EMBO Rep 2002a;3:165–170. [PubMed: 11818333]

Vasseur S, Hoffmeister A, Garcia-Montero A, Mallo GV, Feil R, Kuhbandner S, Dagorn JC, Iovanna JL. p8-deficient fibroblasts grow more rapidly and are more resistant to adriamycin-induced apoptosis. Oncogene 2002b;21:1685–1694. [PubMed: 11896600]

Vasseur S, Vidal Mallo G, Fiedler F, Bodeker H, Canepa E, Moreno S, Iovanna JL. Cloning and expression of the human p8, a nuclear protein with mitogenic activity. Eur J Biochem 1999;259:670–675. [PubMed: 10092851]

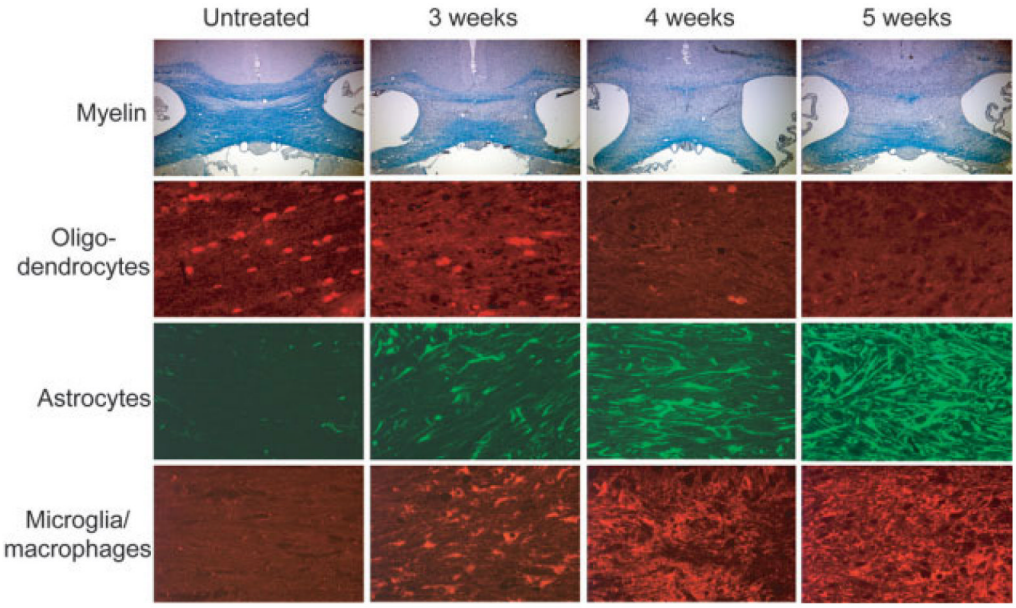

Fig. 1.

Time course of cuprizone-induced inflammation and demyelination. In an untreated state (left column), the corpus callosum is fully myelinated as assessed by LFB-PAS staining and GSTπ^+ mature oligodendrocytes are abundant. Very few to no GFAπ^+ astrocytes and lectin$^+$microglia/macrophages are detected in this region. After 3 weeks of cuprizone treatment (second column), significant demyelination occurs in the corpus callosum. Significant oligodendrocyte loss occurs by 3 weeks, while astrocytes and microglia begin to populate this area. After 5 weeks of cuprizone treatment, the corpus callosum is devoid of myelinated axons, and no GSTπ^+mature oligodendrocytes are detected. Astrogliosis and microglial/macrophage infiltration becomes more prominent between 3 and 5 weeks.

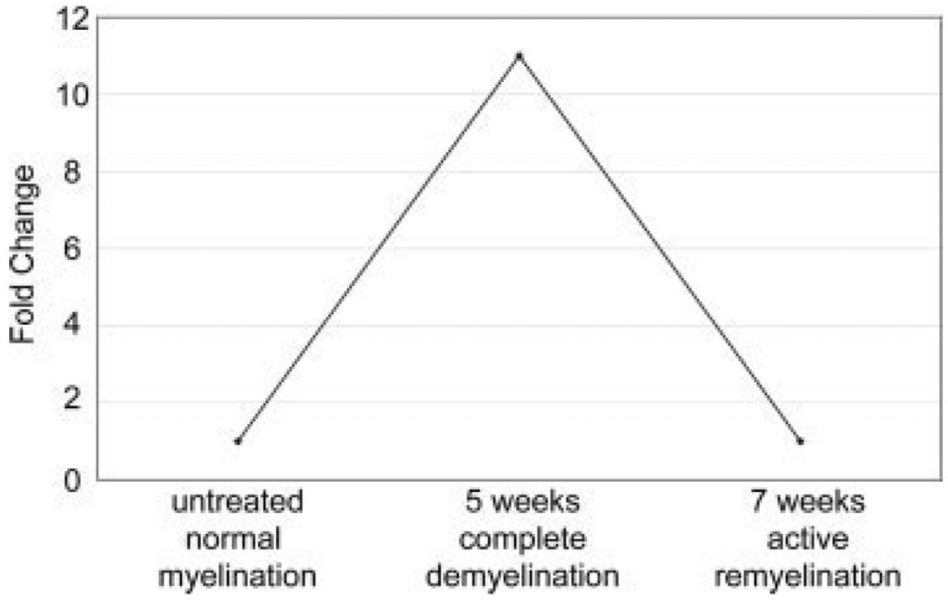

Fig. 2.

Upregulation of p8 during cuprizone-induced demyelination. Affymetrix GeneChip analysis shows that p8 expression was increased 11X following 5 weeks of cuprizone treatment when compared with the untreated brain. One week after removal of cuprizone from the diet of mice (7 weeks), remyelination occurs, and p8 levels returned to baseline.

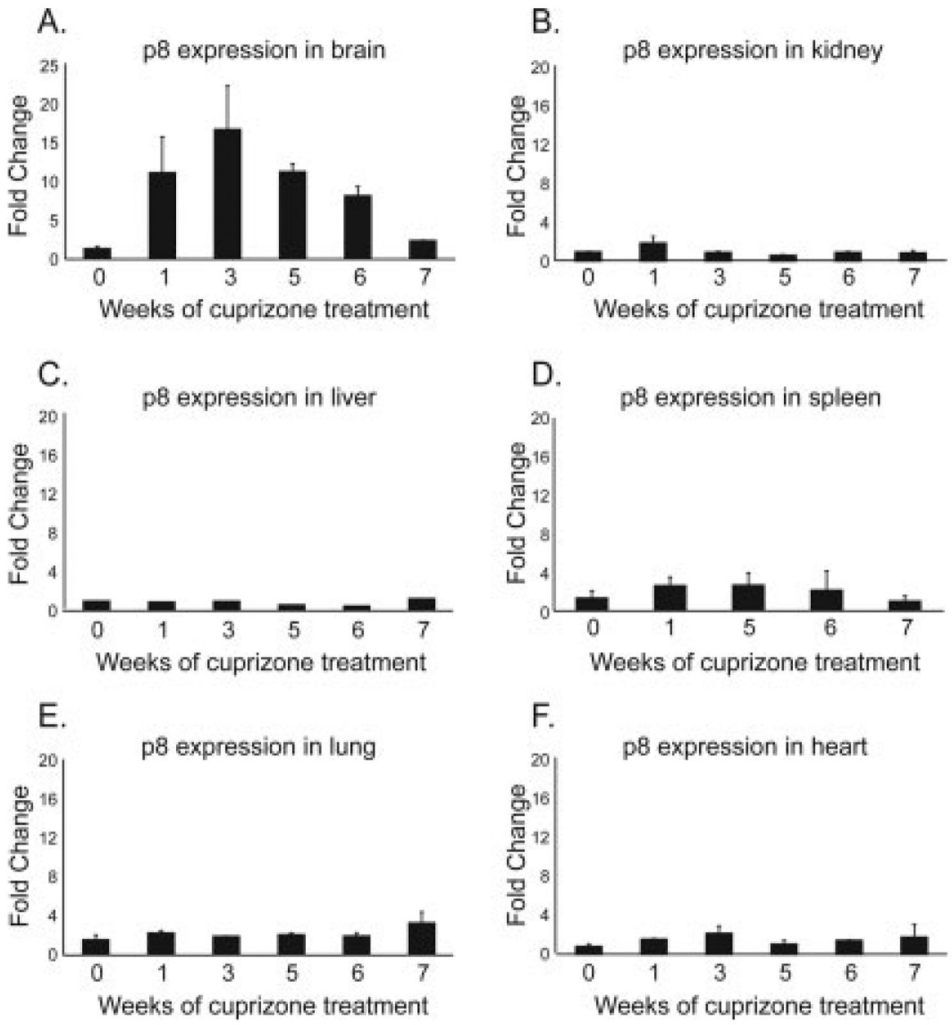

Fig. 3.

Cuprizone-induced p8 upregulation is restricted to brain tissues. Real-time PCR analysis of p8 mRNA levels in tissue following 1, 3, 5, or 6 weeks of cuprizone treatment was performed. The 7-week time point is 1 week after removal of cuprizone from the diet. Data were standardized to 18S and is expressed as fold change over the untreated state. **A:** Brain was the only location where p8 was upregulated during cuprizone treatment. p8 mRNA reverted to pretreatment levels by 7 weeks. Levels of p8 mRNA in the kidney (**B**), liver (**C**), spleen (**D**), lung (**E**), and heart (**F**) remained similar to the untreated state at all time points. Each bar is the average of three mice.

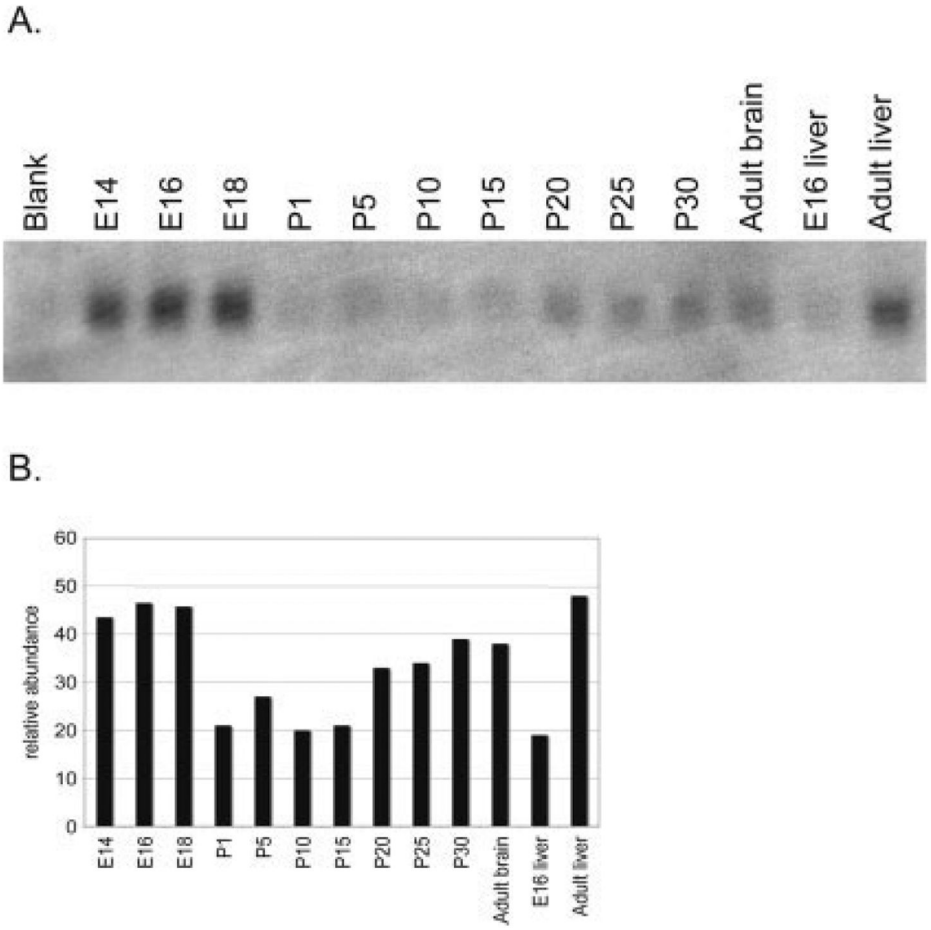

Fig. 4.

Northern blot analysis of p8 in embryonic and postnatal brain and liver. **A:** Levels of p8 were highest in embryonic days 14–18 brain, downregulated at birth, and expressed at a low but detectable level in the adult CNS. **B:** Expression of p8 and beta-actin (data not shown) were quantitated using NIH Image 1.62 software, and relative abundance of p8 was determined.

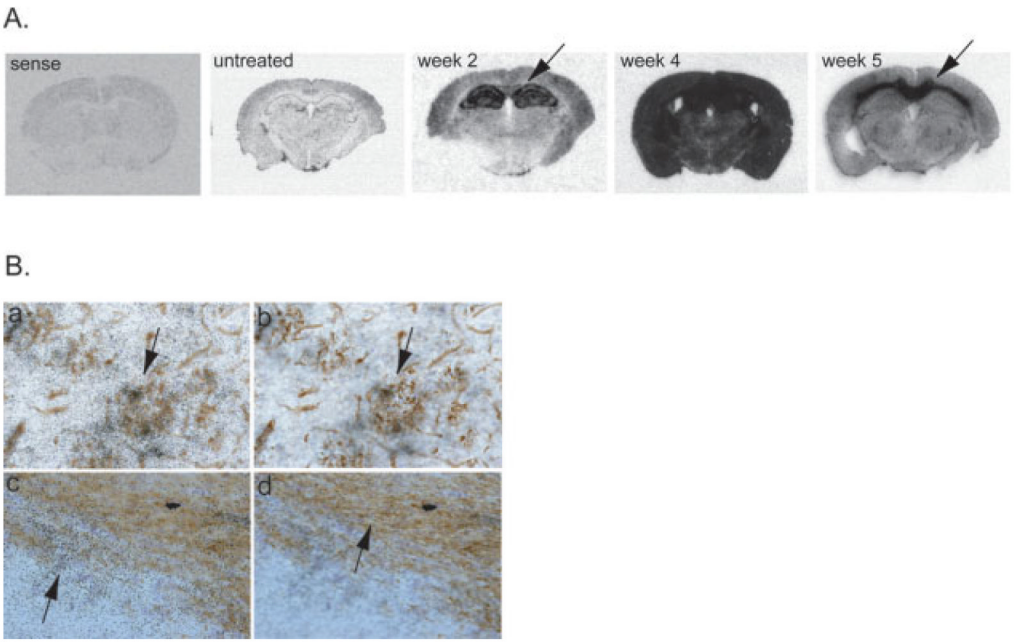

Fig. 5.

Localization of p8 in cuprizone treated brain. In situ hybridization analysis coupled with immunohistochemistry was performed on untreated and cuprizone treated brains. **A:** Whole brain images demonstrate the temporal differences in p8 expression over the course of cuprizone treatment. Sections hybridized with the sense p8 probe show no staining (sense). All other brain sections were labeled with the p8 antisense riboprobe. **B:** Biotinylated tomato lectin (a,b) was used to label microglia and macrophages in the corpus callosum after 4 weeks of cuprizone treatment. CNPase-specific antibodies were used to label oligodendrocytes (c,d) in the hippocampus after 4 weeks of cuprizone treatment. All cell types were visualized in brown. p8 expression was detected using ^{33}P-labeled riboprobes and visualized as black grains in photoemulsion. **a,b:** Two focal planes of the same tissue section. **a:** Focus on the level of the grains in the photoemulsion while in panel b, the focus is on the level of lectin-positive microglia. These panels demonstrate p8 co-localizes with lectin-positive microglia (arrows). **c,d:** Two focal planes of the same tissue section. **c:** Focus on the level of the grains in the photoemulsion. **d:** In contrast, focus is on the level of the CNPase immunohistochemistry. There was very little colocalization of p8 and CNPase.

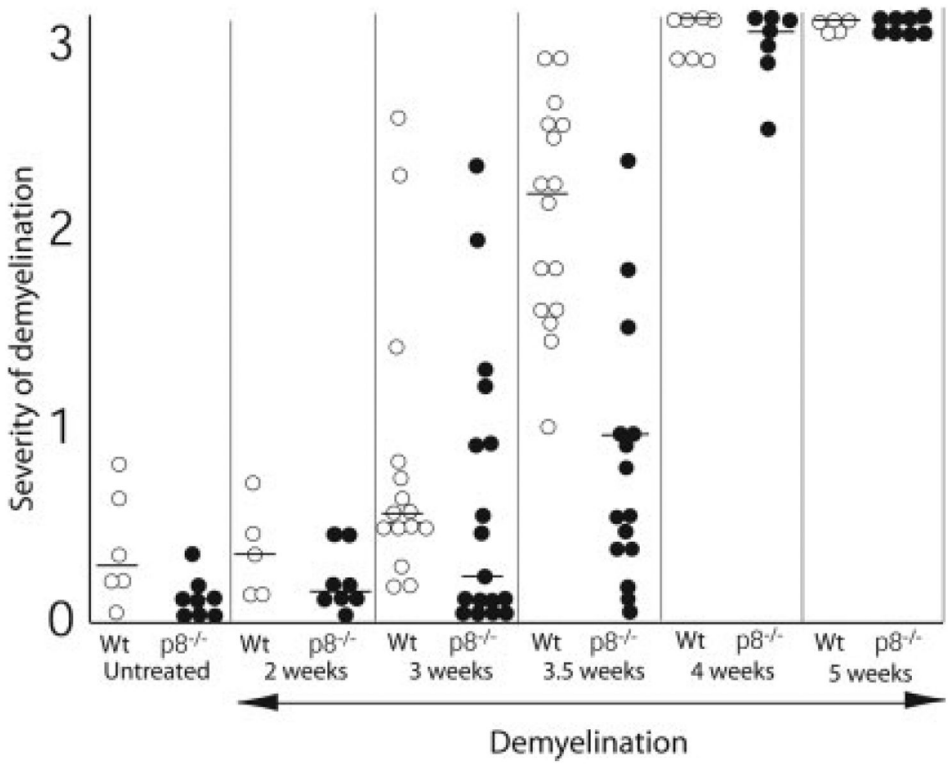

Fig. 6.

Delay in demyelination in p8$^{-/-}$ mice. LFB stained brain sections from p8$^{-/-}$ and wild-type mice were graded on a scale from 0 (complete myelination) to 3 (complete demyelination) by 3 double-blinded investigators. White circles represent p8$^{-/-}$ mice and black circles represent wild-type mice. Horizontal lines represent the median in each group. A significant delay in demyelination in p8$^{-/-}$ mice is found at the 3.5-week time point. The toxicity of cuprizone treatment results in complete demyelination in all mice by 4–5 weeks of cuprizone treatment.

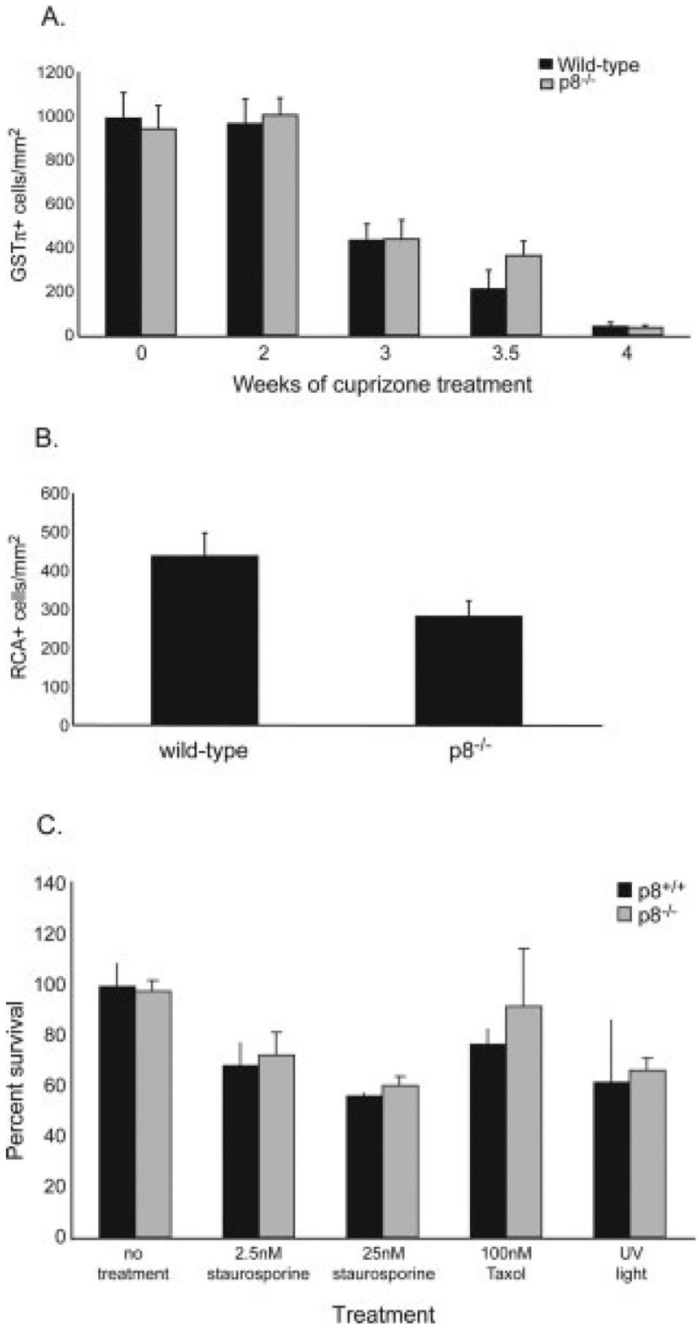

Fig. 7.

Reduced numbers of mature oligodendrocytes and less CNS microglial/macrophage infiltration in $p8^{-/-}$ mice. A. GSTπ immunohistochemistry was performed on paraffin sections from untreated and 2-, 3-, 3.5-, and 4-week treated brain. $GST\pi^{+}$ cells at midline corpus callosum were quantitated. No differences in the numbers of oligodendrocytes in the untreated state or after 2 or 3 weeks of cuprizone treatment were observed. Less oligodendrocytes are found in wild-type mice compared with $p8^{-/-}$ mice after 3.5 weeks of treatment, although not statistically significant. By week 4, almost no oligodendrocytes are detected in the corpus callosum in either $p8^{-/-}$ or wild-type mice. B. Paraffin brain sections from wild-type and $p8^{-/-}$ mice treated for 3.5 weeks were stained with RCA-1 lectin. RCA^{+} cells at midline corpus

callosum were quantitated. Significantly fewer microglia/macrophages were found in the $p8^{-/-}$ mice ($P < 0.04$). **C:** Absence of p8 does not affect cell viability in response to a variety of apoptotic stimuli. Peritoneal macrophages were isolated from $p8^{-/-}$ or wild-type control mice. After 12 h, the media was replaced with media containing the indicated concentrations of staurosporine or Taxol. As an additional treatment, one set of wells was exposed to UV radiation for 10 min. Cell viability was measured 72 h later using the XTT assay. No significant difference in death was observed between control and $p8^{-/-}$macrophages.

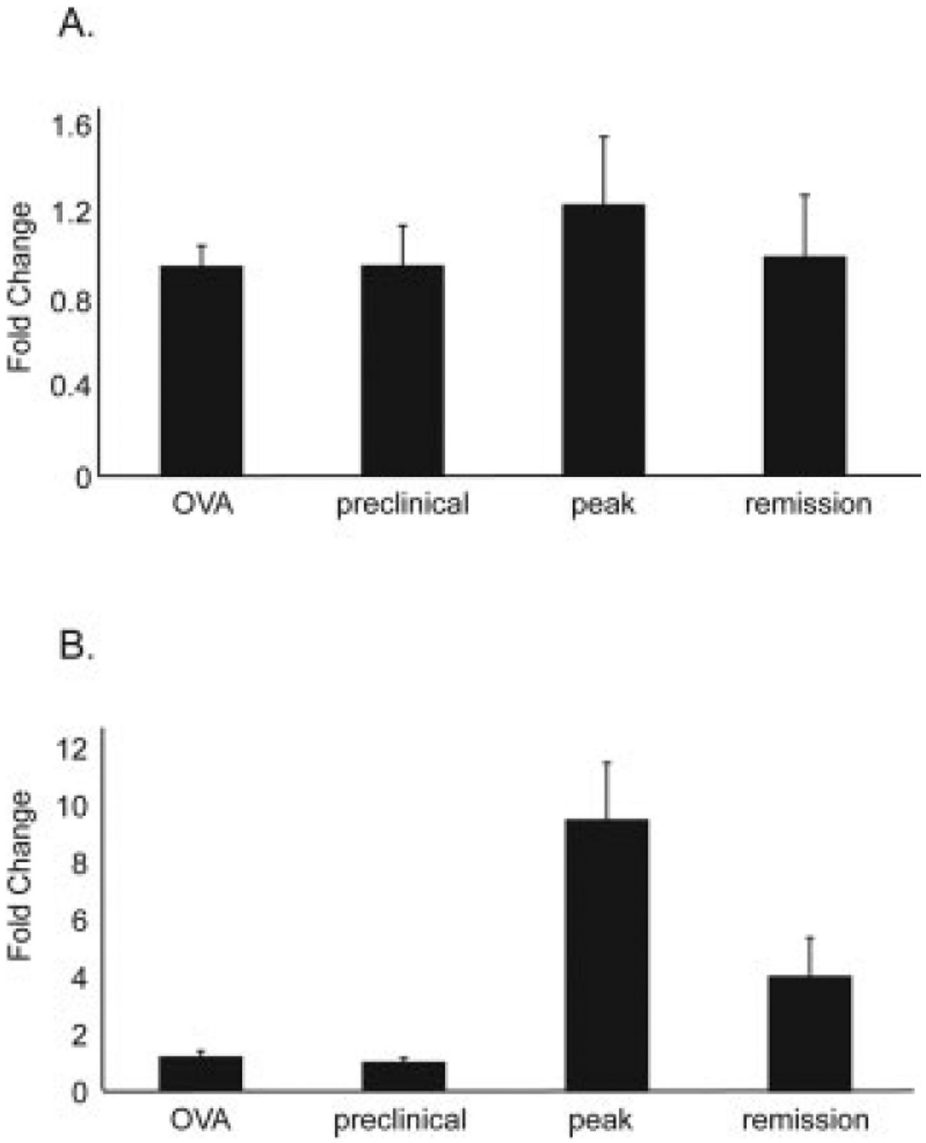

Fig. 8.

p8 upregulation in experimental autoimmune encephalomyelitis. Wild-type SJL mice were immunized with OVA or $PLP_{139–151}$ and adjuvant. Immunized mice were sacrificed at one of three clinical time points. Brain and spinal cords were removed for real-time PCR analysis of p8 mRNA levels. **A:** p8 mRNA levels in the brains of $PLP_{139–151}$ immunized mice did not change over the clinical time course, nor were they different from p8 levels in the brains of OVA immunized mice. B: p8 mRNA levels in the spinal cords of $PLP_{139–151}$ immunized mice were not different from OVA immunized mice at the preclinical stage. However, a significant increase in p8 was found in the spinal cord at the peak of EAE in $PLP_{139–151}$ immunized mice. In the clinically defined remission stage, p8 levels fall but remain elevated above the preclinical state.

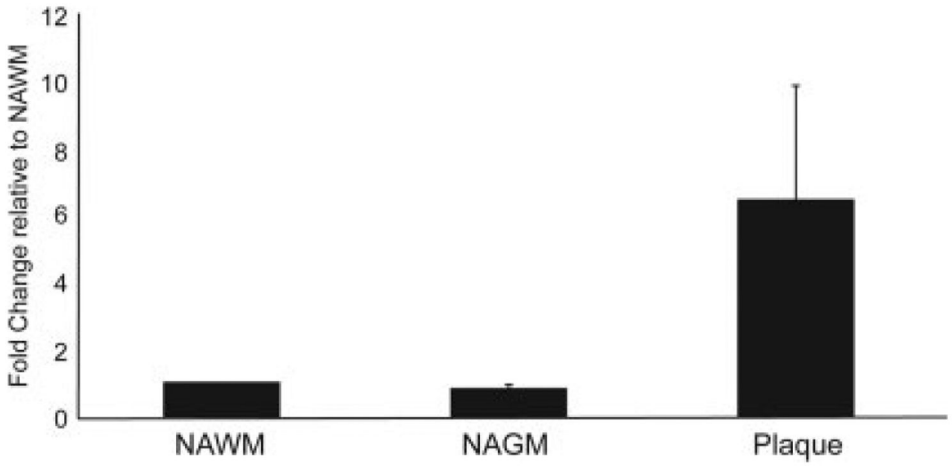

Fig. 9.

Upregulation of p8 in multiple sclerosis plaques. Real-time PCR analysis was performed on cDNA generated from postmortem brain tissue from MS patients. Normal-appearing white matter (NAWM) and normal-appearing gray matter (NAGM), found adjacent to plaques, were analyzed. Compared with NAWM, the p8 mRNA levels in plaques were significantly elevated, while NAGM was not different from NAWM.